Biol. Cell (2012) **104**, 213–228 DOI: 10.1111/boc.201100070

Research article

TI-VAMP/VAMP7 is the SNARE of secretory lysosomes contributing to ATP secretion from astrocytes

Claudia Verderio*[1], Cinzia Cagnoli*†, Matteo Bergami‡, Maura Francolini*†, Ursula Schenk*[2], Alessio Colombo*, Loredana Riganti*, Carolina Frassoni‖, Emanuela Zuccaro‡, Lydia Danglot§¶, Claire Wilhelm#, Thierry Galli§¶, Marco Canossa‡ and Michela Matteoli*^[1]

*Department of Medical Pharmacology and CNR Institute of Neuroscience, Università di Milano, 20129 Milan, Italy, †Fondazione Filarete, 20139 Milan, Italy, ‡Department of Neuroscience and Brain Technologies, Italian Institute of Technology, 16163 Genoa, Italy, ‖Epileptology and Experimental Neurophysiology Unit, Fondazione IRCCS Istituto Neurologico "Carlo Besta", Milan, Italy, §Membrane Traffic in Neuronal and Epithelial Morphogenesis, INSERM U950, 75013 Paris, France, ¶Institut Jacques Monod-CNRS UMR7592, Université Denis Diderot Paris 7, 75013 Paris, France, #Laboratoire Matière et Systèmes Complexes (MSC), UMR 7057 CNRS and University Paris Diderot, Paris, France, and ^IRCCS Istituto Clinico Humanitas, Rozzano, Milan, Italy

Background information. ATP is the main transmitter stored and released from astrocytes under physiological and pathological conditions. Morphological and functional evidence suggest that besides secretory granules, secretory lysosomes release ATP. However, the molecular mechanisms involved in astrocytic lysosome fusion remain still unknown.

Results. In the present study, we identify tetanus neurotoxin-insensitive vesicle-associated membrane protein (TI-VAMP, also called VAMP7) as the vesicular SNARE which mediates secretory lysosome exocytosis, contributing to release of both ATP and cathepsin B from glial cells. We also demonstrate that fusion of secretory lysosomes is triggered by slow and locally restricted calcium elevations, distinct from calcium spikes which induce the fusion of glutamate-containing clear vesicles. Downregulation of TI-VAMP/VAMP7 expression inhibited the fusion of ATP-storing vesicles and ATP-mediated calcium wave propagation. TI-VAMP/VAMP7 downregulation also significantly reduced secretion of cathepsin B from glioma.

Conclusions. Given that sustained ATP release from glia upon injury greatly contributes to secondary brain damage and cathepsin B plays a critical role in glioma dissemination, TI-VAMP silencing can represent a novel strategy to control lysosome fusion in pathological conditions.

Introduction

Recent evidence has demonstrated more active roles of glial cells in brain pathophysiology than previously thought. Consequently, a novel view of the brain function has emerged in which brain physiology results from the interactive activity of neuron–glial networks. Astrocytes represent the main population of glial cells in the central nervous system (CNS). They have recently gained attention because they have an important function in the formation and activity of synapses under normal or pathological conditions. In the adult brain, astrocytes respond to synaptic activity by $[Ca^{2+}]_i$ elevations, driven by activation of different neurotransmitter receptors, and propagate calcium signals which may be transmitted over significant distances, thus participating in integrative processes in the CNS. Calcium elevations in astrocytes lead to the release of various gliotransmitters,

[1]Correspondence may be addressed to either of these authors (email c.verderio@in.cnr.it, michela.matteoli@unimi.it).
[2]Present address of Ursula Schenk is Pharmanalytica SA, Via S. Balestra 31, Locarno CH-6601, Switzerland.
Key words: Astrocytes, ATP, Cathepsin B, Secretory lysosomes, TI-VAMP/VAMP7.
Abbreviations used: cDNA, complementary DNA; CNS, central nervous system; DS red, Discosoma red fluorescent protein; GFAP, glial fibrillar acidic protein; GFP, green fluorescence protein; SDS-PAGE, sodium dodecyl sulphate-polyacrylamide gel electrophoresis; Sg II, secretogranin II; t-ACPD, trans-1-aminocyclopentane-1,3-dicarboxylic acid; TeNT, tetanus toxin; TfR, transferrin receptor; TIRF, total internal reflection fluorescence; TI-VAMP, tetanus neurotoxin-insensitive vesicle-associated membrane protein; t-SNARE, target SNARE; v-SNARE, vesicular SNARE.

including glutamate, D-serine, ATP and peptides, that can signal back to neurons, thus modulating neurotransmission (Fellin, 2009; Montana et al., 2006) but the molecular and cellular mechanisms involved are still debated (Hamilton and Attwell, 2010). Unconventional pathways, involving microvesicle shedding from the plasma membrane, are also active in glial cells and mediate the release of cytokines (Bianco et al., 2009).

Two main mechanisms of release of small transmitters have been defined: (i) a direct loss of the chemical transmitters from the cytoplasm into the extracellular medium, mediated by anion channels, connexin hemichannels, $P2X_7$ receptor channels and transporter proteins, which is favoured in conditions such as ischemia, traumatic injury and seizure activity (Evanko et al., 2004; Hamilton and Attwell, 2010) and (ii) a regulated form of exocytosis, mediated by clear vesicles, with a diameter of 30–100 nm, deputed to the release of glutamate and D-serine (Bezzi et al., 2004; Crippa et al., 2006; Mothet et al., 2005; Zhang et al., 2004), large dense core vesicles, which store secretogranin II (Sg II) (Calegari et al., 1999; Hur et al., 2010) peptides (ANP) and a fraction of cellular ATP (Coco et al., 2003; Pangrsic et al., 2007; Parpura and Zorec, 2010; Pascual et al., 2005; Pryazhnikov and Khiroug, 2008; Ramamoorthy and Whim, 2008; Striedinger et al., 2007) and secretory lysosomes (Jaiswal et al., 2007; Li et al., 2008; Zhang et al., 2007) which contain ATP but not glutamate. On the basis of live cell imaging, it was recently proposed that lysosomes are the major vesicular compartment undergoing calcium-regulated exocytosis from cortical astrocytes (Li et al., 2008). A marker of secretory lysosomes is the vesicular SNARE tetanus neurotoxin-insensitive vesicle-associated membrane protein (TI-VAMP, also called VAMP7) (Casey et al., 2007; Proux-Gillardeaux et al., 2007; Rao et al., 2004). TI-VAMP is a member of the vesicular SNARE proteins (v-SNAREs) which interact with target SNAREs (t-SNAREs) to form the so-called SNARE complex which plays a central role in the fusion mechanism. Upon calcium elevation, TI-VAMP forms SNARE complexes in non-neuronal cells with SNAP-23 and syntaxin 3 or 4 (Rao et al., 2004), which are the prevalent isoform expressed in astrocytes both in culture and *in situ* (Hepp et al., 1999; Paco et al., 2009; Schubert et al., 2011). TI-VAMP is present also in neurons, where it drives neuritogenesis. Although previous studies showed that TI-VAMP is expressed in astrocytes, the precise nature of the TI-VAMP compartment is still not clear (Li et al., 2008; Martineau et al., 2008). A strong correlation between TI-VAMP immunofluorescence and the lysosomal membrane markers CD63 (Li et al., 2008) suggested that also in astrocytes TI-VAMP mediates lysosome exocytosis. We aimed, therefore, at investigating whether TI-VAMP mediates the release of gliotransmitters via the exocytosis of lysosomes.

Results

TI-VAMP supports vesicle fusion with the astrocyte plasma membrane

In line with previous evidence (Li et al., 2008; Martineau et al., 2008), we found that cultured primary astrocytes express TI-VAMP. Figure 1A shows a double immunofluorescence staining of rat primary hippocampal astrocytes for glial fibrillary acidic protein (red) and TI-VAMP (green). TI-VAMP staining displayed a punctuate pattern and was distributed in the perinuclear area and the cell periphery (Figures 1A′ and 1B). To define whether TI-VAMP labelling is also detectable *in situ*, sections of paraformaldehyde-fixed E16 rat cortices were double stained for TI-VAMP (red) and vimentin (green), a well established marker for radial glial fibers. TI-VAMP staining was clearly detectable in the lower region of the ventricular zone where resides the somata of radial glial cells and in the marginal zone where the endfeet of glial fibres processes establish contacts with the pial surface (Figures 1C and 1C″ and high magnification). TI-VAMP immunoreactivity was also detectable in the human astrocytoma cell line ADF (Figure 1G). Interestingly, western blot analysis indicated higher TI-VAMP expression in the glioma cell lines as compared with primary human astrocytes (Figure 1H).

To assess whether TI-VAMP vesicles undergo fusion with the astrocyte plasma membrane, cells were transfected with a complementary DNA (cDNA) coding for TI-VAMP fused to green fluorescent protein (GFP) at the intraluminal C-terminus (Figure 1D, green). Astrocytes were then exposed at 4°C to anti-GFP antibodies, based on the assumption that the antibodies will be able to recognise the GFP

Figure 1 | TI-VAMP-positive organelles in astrocytes undergo fusion with the plasma membrane
(**A** and **A′**) Primary hippocampal astrocytes double labelled for glial fibrillary acidic protein (GFAP; red) and TI-VAMP (green). Inset shows the fluorescence intensity plot of TI-VAMP along the white line. Scale bar: 15 μm. (**B**) Overlay of TI-VAMP staining (green) with the DIC image, which shows TI-VAMP immunoreactivity at the cell border. Scale bar: 12 μm. (**C** and **C′′**) sections of paraformaldehyde-fixed E16 rat cortex double stained for TI-VAMP (red) and vimentin (green). Vimentin immunoreactivity (**C**) is evident in parallel radial glial fibres extending radially from ventricular zone to the pial surface. TI-VAMP staining is detectable in the ventricular zone where resides the oval somata of radial glial cells, and is prominently localised at the endfeet processes which establish contacts with the pial surface (**C′**). Overlap in expression of vimentin and TI-VAMP is shown in yellow (**C′′**). Scale bar: 130 μm. Details of the astrocyte endfeet region are shown below. Scale bar: 20 μm. (**D**) Astrocytes transfected with a cDNA codifying for TI-VAMP fused to GFP at the intraluminal C-ter were exposed at 4°C to anti-GFP antibodies, fixed and stained with secondary antibodies. Fusion of TI-VAMP vesicles, revealed by anti-GFP staining (red), is mainly localised at the free astrocyte surface. Labelling for GFAP (blue) confirms the cell identity as astrocytes. Inset shows the fluorescence intensity plot of over-expressed TI-VAMP along the white line. Scale bar: 14 μm. (**E**) Astrocytes transfected with a cDNA codifying for cellubrevin/VAMP3 fused to GFP at the intraluminal portion, treated as in D. Note that fusion of cellubrevin/VAMP3 vesicles revealed by anti-GFP staining (red) occurs also at cell-to-cell contacts. Scale bar: 13 μm. (**F**) Control astrocytes, transfected with a cDNA codifying for cytoplasmic GFP, negative for anti-GFP staining (red). (**G**) Labelling for endogenous TI-VAMP of ADF cultures. (**H**) Extracts from primary human astrocytes and from the human glioma cell line ADF were analysed by immunoblotting for TI-VAMP expression. Ribophorin staining guarantees for equal protein loading. Note the high level of protein expression in ADF glioma.

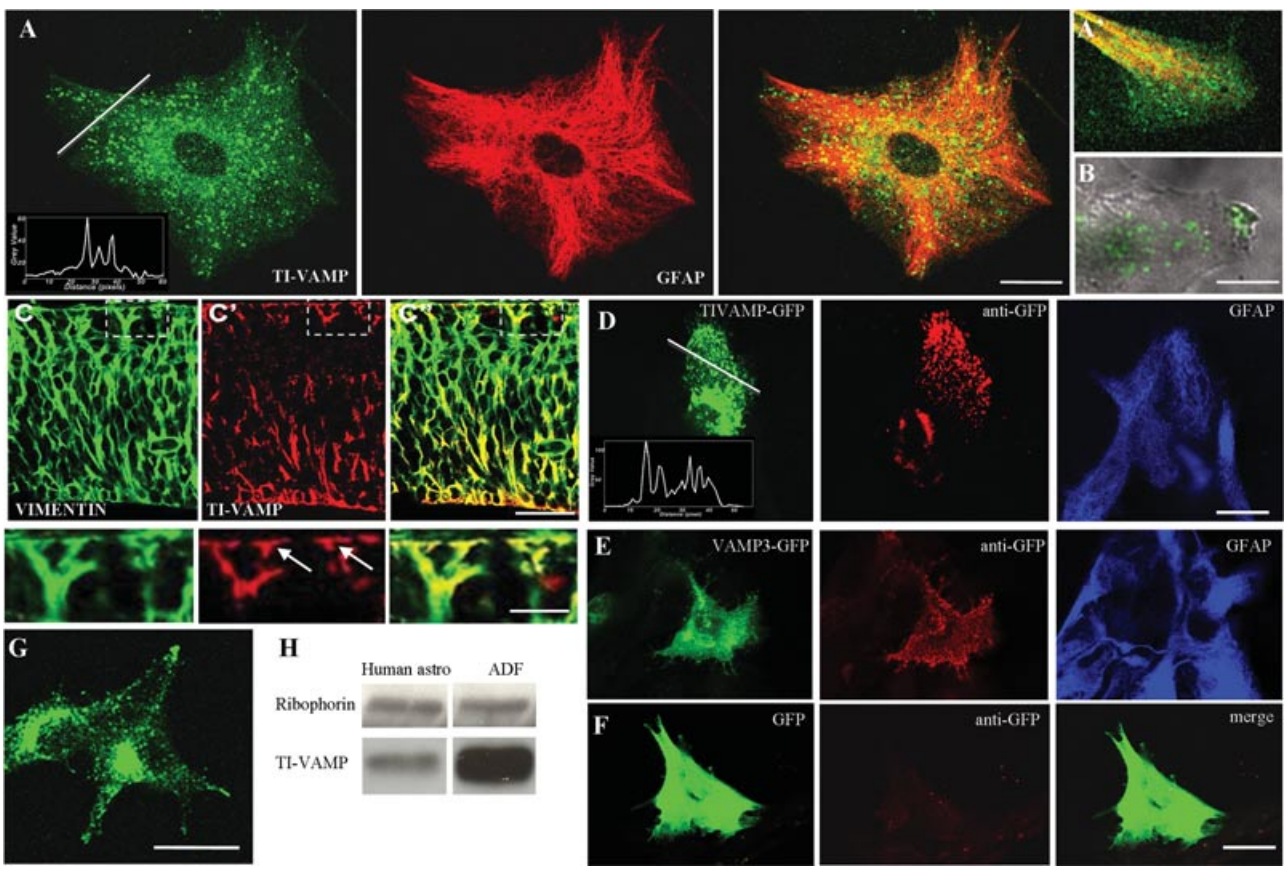

epitope only upon exposure of the epitope to the astrocyte surface, consequently to fusion of the vesicle with the plasma membrane. Figure 1D shows a bright surface labelling of astrocytes with anti-GFP antibodies (red), which indicates sites where the fusion of the vesicles and exposure of the epitope have

Figure 2 | TI-VAMP organelles are distinct from VAMP2 or secretogranin II (SgII)-positive vesicles

(**A** and **B**) Double immunostaining of cultured astrocytes for TI-VAMP (green) and VAMP2 (**A**, red) or Sg II (**B**, red). The merge panels indicate lack of co-localisation between TI-VAMP and either VAMP2 or Sg II. Scale bar: 28 μm in A; 15,5 in B. (**C** and **D**) Details of double labellings between TI-VAMP and VAMP2 (**C**), TI-VAMP and Sg II (**D**). (**E**) Double labelling of TI-VAMP and CD63, showing a high degree of co-localisation between the TI-VAMP and the lysosomal marker. Scale bar: 12 μm. (**F**) Quantitative analysis of co-localisation between TI-VAMP and either VAMP2 or Sg II or CD63. (**G**) Puncta labelled by TI-VAMP-GFP show accumulation of Mant-ATP (red). Scale bar: 5 μm. (**H**) Sucrose equilibrium gradient analysis of relative densities of the vesicles containing TI-VAMP, VAMP3, VAMP2 and SgII in hippocampal astrocytes. The post-nuclear superrnatant from astrocytes was centrifuged through a 0.4–1.8 M sucrose gradients, 22 fractions were collected from the gradient and pelleted in 80% acetone at -20°C. Aliquots of each fraction were analysed by immunoblotting. (**I** and **J**) Examples of astrocytes transfected with cDNA codifying for TI-VAMP fused to a GFP tag, fixed and double stained for the early endosome marker EAA1 (**I**) or for the lysosome markers CD63 (**J**). A partial co-localisation is detectable with the lysosome marker. Scale bar: 7 μm in I; 10 μm in J; (**K**) Double labellings for endogenous TI-VAMP (green) and cathepsin B (red) of ADF cells, showing a clear co-staining of glioma tips. Scale bar: 13 μm. (**L**) Sucrose equilibrium gradient analysis of density distribution of TI-VAMP and cathepsin B in ADF glioma. Cathepsin B appears as the precursor form of 46 kDa and the mature forms of 30 kDa and 25 kDa.

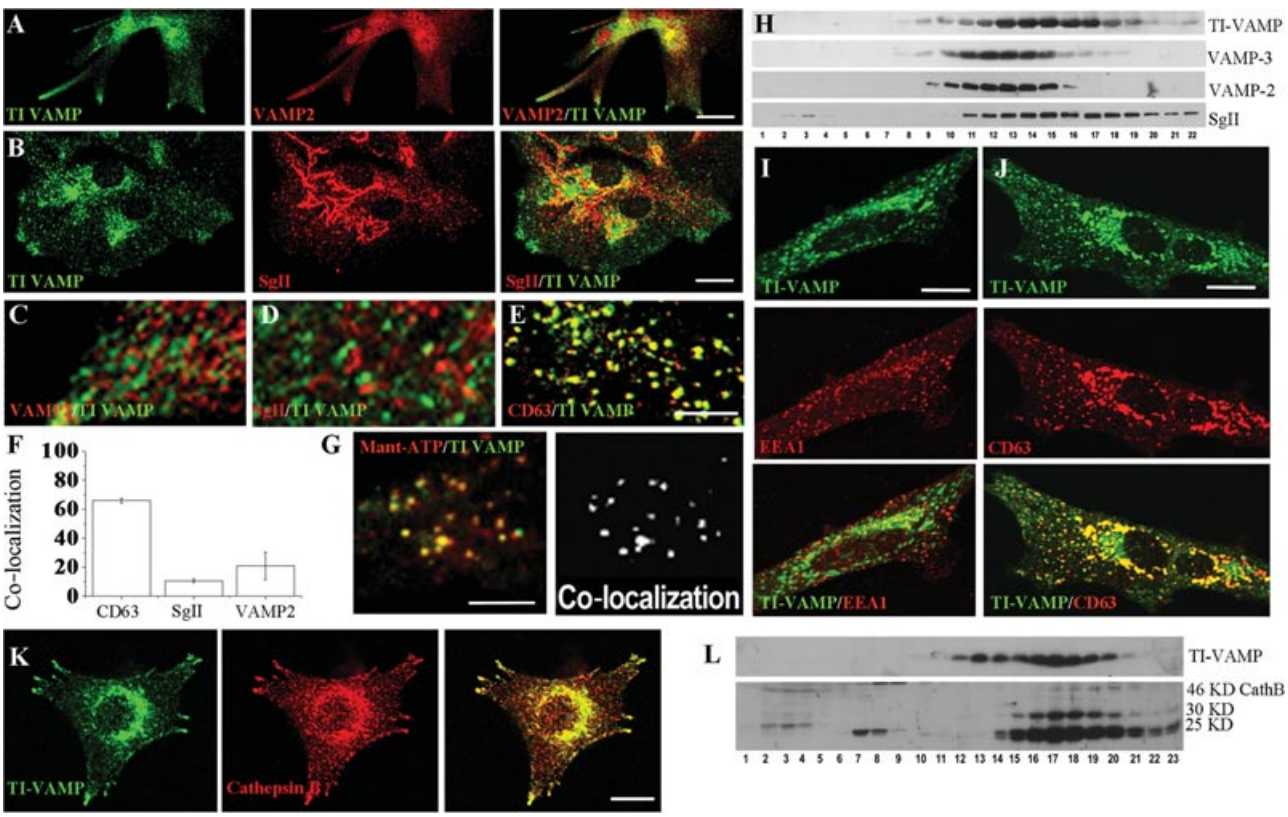

occurred. Interestingly, fusion of TI-VAMP vesicles occurred predominantly at the contact-free cell surface (Figure 1D, red). On the contrary, fusion of cellubrevin/VAMP3 vesicles, detected using a similar luminal GFP-tagged cDNA, occurred homogeneously over the entire plasma membrane (Figure 1E, red). No internalisation of anti-GFP antibodies occurred in control astrocytes transfected with cytoplasmic GFP (Figure 1F).

TI-VAMP vesicles represent an exocytic pathway distinct from VAMP2/VAMP3 or Sg II-positive organelles

We then carried out subcellular fractionation on sucrose equilibrium gradients, and the fractions were probed by western blotting for the clear vesicle markers synaptobrevin/VAMP2 and cellubrevin/VAMP3, for the large dense core vesicle marker Sg II and TI-VAMP (Figure 2H). The bulk of VAMP2 was

recovered, together with VAMP3, in the light sucrose gradient subcellular fractions (fractions 10–15), supporting the evidence that VAMP2 and VAMP3 are localised on the same astrocytic vesicle population (Crippa et al., 2006). VAMP2 and VAMP3 partially overlapped with the Sg II-containing fractions (bulk in fractions 14–19), as previously described (Coco et al., 2003). The majority of TI-VAMP was instead recovered in intermediate density fractions (bulk in fractions 12–17), which largely overlap with Sg II organelles (Figure 2H), suggesting that TI-VAMP-positive fractions may also contain Sg II positive vesicles, enriched in ATP (Coco et al., 2003). However, immunofluorescence stainings of cultured astrocytes showed lack of coincidence between TI-VAMP vesicles and either Sg II or VAMP2 organelles. As shown in Figures 2A and 2B, relative magnifications (Figures 2C and 2D) and quantitative analysis (Figure 2F), TI-VAMP immunoreactivity did not co-localise with either VAMP2 or Sg II stainings. These data support the existence of at least three distinct types of secretory vesicles in astrocytes.

TI-VAMP labels a compartment of late endosomal/lysosomal origin

TI-VAMP has been shown to be involved in fusion processes along the endocytic pathways (Advani et al., 1999; Pryor et al., 2004) and has been indicated as the v-SNARE which mediates secretion of granules of lysosomal nature in several cell types (Casey et al., 2007; Logan et al., 2006; Oishi et al., 2006; Proux-Gillardeaux et al., 2007; Rao et al., 2004; Sander et al., 2008). TI-VAMP fused to GFP was over-expressed by transfection and astrocytes were stained for the early endosome marker EAA1 and for the late endosome–lysosome markers CD63. Figures 2I and 2J show that TI-VAMP poorly co-localised with EAA1, whereas a prominent qualitative co-localisation was detected with CD63, suggesting the endosomal–lysosomal nature of the TI-VAMP compartment in astrocytes. Furthermore, double labelling for endogenous TI-VAMP and CD63 revealed a high degree of co-localisation (Figures 2E and 2F). Consistent with previous evidence indicating that Mant-ATP, a fluorescent nucleotide analogue used for studying ATP stores, labels CD63 positive lysosomes (Zhang et al., 2007), total internal reflection fluorescence (TIRF) analysis of astrocytes transfected with TI-VAMP fused to GFP revealed that TI-VAMP-positive organelles contain ATP (Figure 2G). As TIRF microscopy detects organelles within 110 nm from the plasma membrane, these data suggest proximity to fusion sites of TI-VAMP-positive vesicles. TI-VAMP localisation was then investigated in the human glioma cell line ADF, which expresses the v-SNARE at high extent (Figure 1H). Subcellular fractionation of ADF cells on sucrose equilibrium gradient revealed that a portion of the lysosomal marker cathepsin B, in both its precursor (46 kDa) and mature forms (30 and 25 kDa), was contained in fractions (16–19), which were also positive for TI-VAMP (Figure 2L). In addition, fluorescence microscopy revealed a significant degree of co-localisation between TI-VAMP and cathepsin B, which was particularly evident at the cell periphery of ADF glioma (Figure 2K), consistent with cathepsin B distribution at the leading edge of glioma cells in tumour infiltration. These data suggest that, in glioma cells, TI-VAMP and the lysosomal marker cathepsin B are on the same membrane trafficking pathway.

Immunoisolation of TI-VAMP organelles

To gain insights into the molecular composition of TI-VAMP vesicles, TI-VAMP-positive organelles were immunoisolated from ADF cells, which express high levels of the protein, using beads bound to anti-TI-VAMP antibodies. Electron microscopy of the beads carrying TI-VAMP vesicles revealed that these organelles had a multilamellar appearance, typical of lysosomes ($n = 139$) (Figure 3A). No vesicles were detected on beads coated with control IgG (Figure 3A′). The size of immunoisolated vesicles ranged from 50 to 240 nm, with the most represented diameter being comprised between 125 and 175 nm (Figure 3C), as previously described in other cell types (Bucci et al., 2000; Caplan et al., 2001). Electron microscopy analysis of ADF cells as well as live staining with lysotracker confirmed the presence of organelles with a similar size and appearance in the cell cytoplasm (Figure 3B, arrows and Figures 3B′ and 3B″).

To characterise their molecular composition, TI-VAMP-immunoisolated vesicles were analysed by sodium dodecyl sulphate-polyacrylamide gel electrophoresis (SDS-PAGE) and western blotting. The immunoisolated vesicles were enriched in TI-VAMP, contained negligible amounts of the mitochondrial marker Tom20 and were completely negative for the peroxisomal marker catalase (Figure 3D).

Figure 3 | Morphological and biochemical characterisation of TI-VAMP vesicles from ADF glioma cell line

(**A**) Electron microscopy images showing anti-TI-VAMP antibody-coated beads with bound ADF vesicles. Round, multilamellar organelles represent the virtual totality of TI-VAMP-positive organelles. No vesicles were immunoisolated using control IgG-coated beads (**A**′). (**B**) Electron microscopy images of an ADF cell. Arrows point to multilamellar organelles. Scale bar in A and B = 150 nm. (**B**′) Overlay of DIC image with lysotracker staining (red) in living ADF cells. High magnification of lysotracker positive puncta is shown in B′′. Arrows point to positive puncta in the size range of organelles in B, at the resolution limit of fluorescence (about 1 pixel in size, 120 nm). (**C**) Histogram showing the size distribution (percentage of total) of vesicles bound to TI-VAMP antibody-coated beads ($n = 139$). The actual number of vesicles analysed is reported within the bars. (**D**) Western blot analysis of low speed supernatant, control rabbit IgG (RIgG) and TI-VAMP immunoisolated organelles (TI-VAMP) for TI-VAMP, the mitochondrial marker Tom20, the peroxisomal marker catalase, the late endosomal/lysosomal rab 7 or the early endosomal markers rab5 and transferrin receptor TfR. (**E**) ADF cells were allowed to bind magnetic nanoparticles for 30 min and, after washing, to internalize them for 30 min or 6 h to label early endosomes and late endosomes/lysosomes, respectively. Western blot analysis revealed a progressive co-enrichment of TI-VAMP and cathepsin B in magnetic fractions. (**F**) Cathepsin B detection by western blotting and pro-Cathepsin B detection by ELISA in vesicles immunoisolated by anti-TI-VAMP coated beads compared with rabbit IgG-coated beads. ELISA values are presented as mean of nanograms per millilitre obtained from samples in triplicate, and are representative of three independent experiments. (**G**) Pro-cathepsin B detection by ELISA in the supernatant collected from ADF cells with or without a 15 h pre-treatment with 40 nM tetanus toxin (TeNT). Values are presented as mean ± SEM nanograms per millilitre and are normalised to micrograms of protein. Note that pre-exposure to TeNT does not inhibit pro-cathepsin secretion.

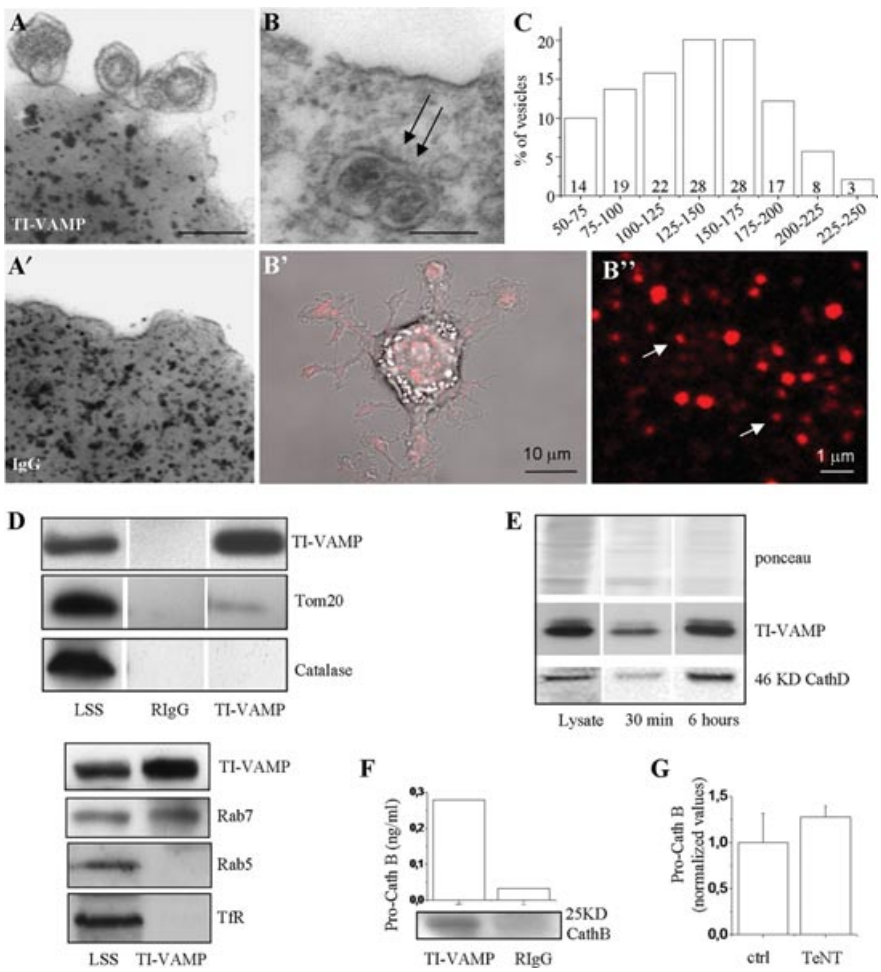

Notably, TI-VAMP-isolated vesicles contained rab7, a marker for late endosomes/lysosomes (Figure 3D, lower panel) and were negative for the early endosomal markers transferrin receptor (TfR) and rab5 (Figure 3D, lower panel). These data indicate that TI-VAMP vesicles are molecularly distinct from VAMP2 clear vesicles, previously characterised in astrocytes, which do not contain TI-VAMP and rab7 (Crippa et al., 2006), and from early endosomes, which are known to contain rab5 and TrfR. Recent studies have shown that anionic magnetic nanoparticles bind to the plasma membrane and are internalised into the cells, accumulating, upon prolonged incubation, into late endosomes–lysosomes (Loubery et al., 2008). To probe the lysosomal nature of TI-VAMP-positive organelles, we attempted to separate lysosomes from ADF cells, upon cell loading with magnetic particles. Interestingly, western blot analysis of magnetic fractions showed that TI-VAMP is co-enriched together with the lysosomal marker cathepsin D in lysosome-enriched fractions, isolated after 6 h internalisation of the magnetic nanoparticles (Figure 3E). To assess further whether TI-VAMP-positive vesicles store cathepsin B, TI-VAMP immunoisolated vesicles were probed for cathepsin B by western blotting and enzyme-linked immunosorbent assay (ELISA) for the pro-enzyme (Figure 3F). The results showed that cathepsin B and pro-cathepsin B are cargoes of TI-VAMP vesicles. In line with the presence of cathepsin B in TI-VAMP-positive vesicles, pro-cathepsin B secretion from glioma cells was resistant to the treatment of the cultures with TeNT (Figure 3F).

Downregulation of TI-VAMP expression inhibits exocytosis of quinacrine-loaded vesicles

Having established the existence of organelles of the endosomal–lysosomal pathway positive for the SNARE TI-VAMP, we aimed at defining the functional impact of TI-VAMP downregulation in astrocytes. The expression of TI-VAMP was reduced by the addition of a small interfering RNA (siRNA) designed for rat TI-VAMP (r-siRNA1) applied for 4 days (Figure 4A). Quantitative analysis of TI-VAMP downregulation relative to control astrocytes or astrocytes treated with negative control oligonucleotides (siNEG) revealed a reduction of the protein expression of about 65% (Figure 4B). Immunocytochemical analysis revealed that reduction of TI-VAMP expression occurred quite homogenously amongst all cells (not shown). Given TI-VAMP is present in lysosomes and ATP is stored and released from secretory lysosomes (Zhang et al., 2007), we investigated whether reduction of TI-VAMP expression impacts ATP release from astrocytes. TIRF microscopy has been previously used to follow exocytosis of vesicles containing ATP, labelled by quinacrine, in cultured astrocytes (Pangrsic et al., 2007; Pryazhnikov and Khiroug, 2008). By TIRF microscopy, we observed that quinacrine accumulates in TI-VAMP-Discosoma red fluorescent protein (DS red) organelles (84.3% of co-localisation after a 15 min incubation; $n = 6$; Figure 4C). These results confirmed that a large fraction of ATP storing vesicles, which are located in the close vicinity (within 70–110 nm) of the plasma membrane, are TI-VAMP positive (see also Figure 2G). Challenging of astrocytes with the agonist of metabotropic glutamate receptor trans-1-aminocyclopentane-1,3-dicarboxylic acid (t-ACPD) induced dequenching flashes caused by the rapid increase in pH upon diffusion of quinacrine to the extracellular medium (Figures 4D and 4E). Only when quinacrine fluorescence increased, spread, and subsequently declined, flashes were considered exocytic events. Quantitative analysis of quinacrine flashes demonstrated that t-ACPD induced a 8.4-fold increase in ATP exocytic events with respect to the control solution ($n = 12$; Figure 4G). Of note, the exocytosis of quinacrine vesicles upon t-ACPD stimulation was reduced up to 75% in TI-VAMP silenced cultures but not in astrocytes treated with siNEG ($n = 4$; Figure 4G). No major difference in the timing of fusion events was envisaged between control and silenced astrocytes, with most events occurring within the first 1–3 s after t-ACPD application. Also, TI-VAMP downregulation did not induce a significant change in the distribution of quinacrine-positive organelles (Figure 4H). Analysis of the submembrane Ca^{2+} signals occurring at quinacrine vesicle fusion sites was performed by TIRF microscopy using the Ca^{2+} indicator X-rod. Ca^{2+} signals were analysed both under basal conditions and upon t-ACPD exposure. We retrospectively analysed only those regions (regions of interest or ROIs) where labelled vesicles had produced a flash upon t-ACPD stimulation, thus defining the spatial–temporal characteristics of individual submembrane Ca^{2+} signals leading to vesicle fusion. Fluorescence traces were analysed in small equal-sized (8 μm^2) squared regions surrounding vesicles fusion.

Figure 4 | TI-VAMP silencing reduces fusion of quinacrine vesicles

(**A** and **B**) western blot analysis of TI-VAMP levels in control cultures and cultures treated with TI-VAMP r-siRNA or control oligonucleotides (siNEG) for 86 h (200 nM). Ribophorin staining guarantees for equal protein loading. TI-VAMP r-siRNA treatment significantly reduces TI-VAMP expression, as quantified in (**B**). (**C**) Images (three times magnification) from a region of interest (white rectangle) document a representative astrocyte transfected with TI-VAMP- DS red 15 min after incubation with quinacrine (green). Bar, 10 μm. (**D**) Representative TIRF images of astrocytes incubated with quinacrine for 15 min. The sequence depicts exocytic fusion (arrows) in selected astrocytic areas before (2 s) and after (6, 9.5, 18 s) t-ACPD perfusion. Bars, 5 μm. (**E**) Left, schematic representation of TIRF microscopy. The arrow represents the excitation laser at the reflecting angle (θ) producing an evanescent wave that penetrates for 70–110 nm in depth. Right, changes in fluorescence intensity of the same vesicles as in panel D. Fluorescence intensity is measured in a circular mask (red circles of panel D) centred over the vesicles. (**F**) Sub-membrane $[Ca^{2+}]_i$ increases during exocytic fusion of labelled vesicles analysed by the calcium indicator X-rod. Sequential images in lower panels depict changes in fluorescence intensity of a single vesicle fusing to the plasma membrane. Seconds indicate time of appearance, increase in brightness and decrease of the fluorescent signals following the stimulus. Bar, 2 μm. Graphs on the right document dequenching flashes of quinacrine fluorescence and $[Ca^{2+}]_i$ in ROI 1-3 before and after t-ACPD application. (**G**) Quantification of fusion events (flashes) after t-ACPD application. The graphic shows the total number of flashes per astrocyte incubated with of without r-siRNA or control oligonucleotides (siNEG). Data represent means $\pm$ SE. (**H**) Representative confocal images of control and TI-VAMP silenced astrocytes (r-siRNA) incubated for 30 min with quinacrine to label intracellular ATP stores and with the lypophilic dye FM 4-64 immediately before acquisition, to label the cell membrane. (**I**) Quantitative analysis of bradykinine-induced ATP release by luciferin/luciferase assay from control astrocytes, TI-VAMP-silenced astrocytes and TI-VAMP-silenced astrocytes transfected with human TI-VAMP resistant to r-siRNA. Bioluminescence data from one representative experiment are shown ($N = 2$), normalised to protein content. TI-VAMP protein expression in the same samples is shown in (**J**). Calnexin staining guarantees for equal protein loading.

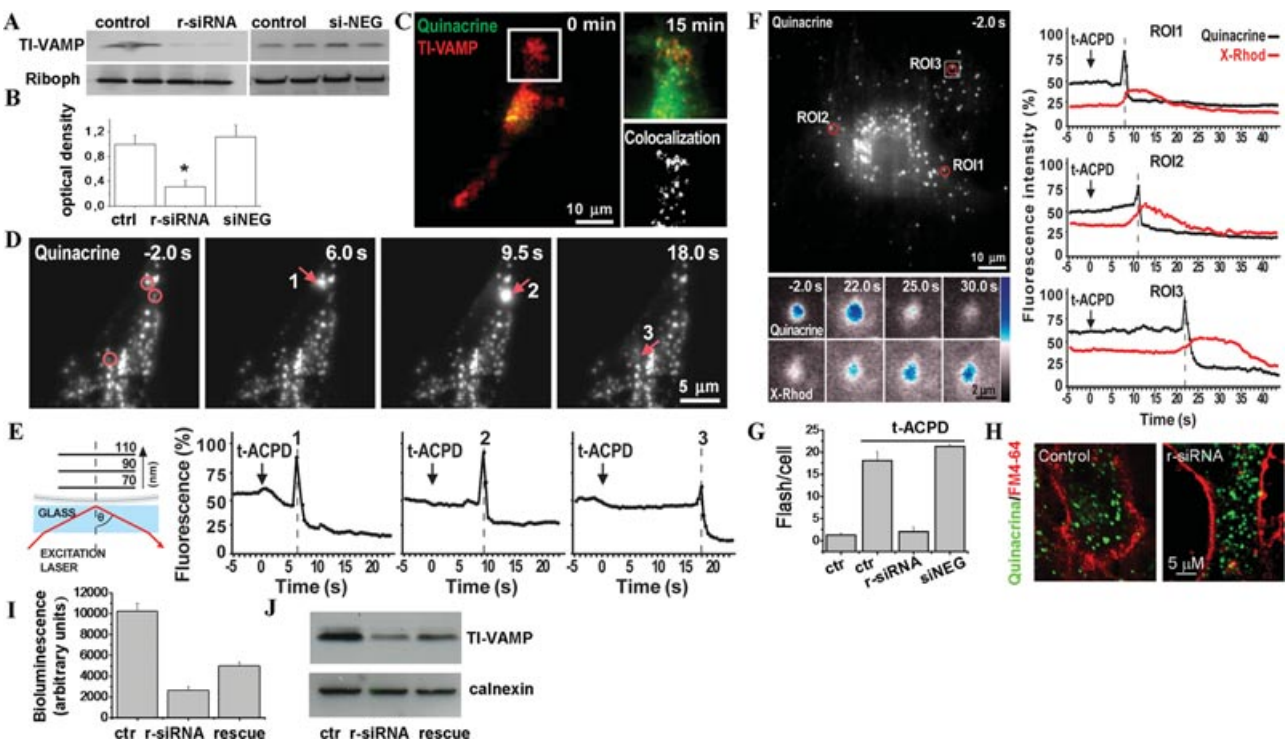

As shown in Figure 4F, rapid increase in fluorescence was easily distinguishable at the time or immediately preceding fusion of vesicles with the plasma membrane. By analysing quinacrine-labelled vesicles and X-rod fluorescence, we observed that, after the stimulation, high Ca^{2+} signal was spread around the fusing vesicle reaching the maximum intensity in close vicinity of the vesicle. Overall, these data

indicate that t-ACPD stimulation induces elevation of submembrane Ca^{2+} that triggers quinacrine-labelled vesicle fusion.

To directly evaluate the contribution of TI-VAMP vesicles to ATP secretion, we measured ATP release by the luciferin–luciferase assay from control astrocytes, r-siRNA-treated astrocytes and r-siRNA-treated astrocytes transfected with human TI-VAMP resistant to r-siRNA. Downregulation of TI-VAMP potently inhibited ATP release, whereas transfection of human TI-VAMP resistant to r-siRNA partially rescued this reduction (Figures 4I and 4J).

Downregulation of TI-VAMP expression reduces calcium wave propagation amongst astrocytes

To further assess the contribution of TI-VAMP vesicles to ATP secretion, we analysed the amplitude and the kinetics of calcium wave propagation induced in cultured astrocytes by mechanical stimulation. Astrocytic calcium waves are dependent on both an intercellular gap-junction pathway, involving calcium and IP3, and an extracellular pathway, involving ATP and/or glutamate. However, in the presence of the gap-junction blocker anandamide (100 μM), ATP release represents the main factor controlling propagation of calcium wave in hippocampal cultures (Figures 5C–5E) (Coco et al., 2003). Analysis of calcium waves in control- and siRNA-treated cultures revealed that TI-VAMP silencing decreases the amplitude (Figure 5H) and the velocity (Figure 5I) of calcium signal (number of analysed fields from three independent experiments: $n = 29$ control, $n = 43$ siRNA; Table 1). No significant alteration of calcium wave propagation was detected in astrocytes treated with siNEG (number of analysed fields: control: $n = 29$, three independent experiments; siNEG, $n = 17$, two independent experiment; Table 1). We could not perform a rescue experiment using r-siRNA-resistant TI-VAMP because of the low efficiency of astrocyte transfection. Nevertheless these data, together with results obtained by direct measurements of ATP by the luciferin–luciferase assay, indicate that TI-VAMP vesicles significantly contribute to ATP release.

Downregulation of TI-VAMP expression reduces cathepsin B secretion from gliomas

We next silenced TI-VAMP expression in ADF glioma to assess the functional impact of the SNARE downregulation. The expression of TI-VAMP was significantly reduced 48 h after addition of a siRNA designed for human TI-VAMP (h-siRNA1) (Figure 6A) as compared with either control cells or cells treated with siNEG. Exposure to h-siRNA1 for additional 48 h almost completely silenced TI-VAMP expression, as indicated by western blotting (Figure 6A) and immunofluorescence staining (Figure 6C). A similar reduction was obtained with a different siRNA (h-siRNA2) (Figure 6A). TI-VAMP downregulation did not alter pro-cathepsin B and cathepsin B expression (Figure 6B), whereas the enzyme immunoreactivity appeared slightly redistributed towards the cell periphery (Figure 6C). Pro-cathepsin B detection by ELISA in the supernatant revealed a significant reduction of the enzyme release in h-siRNA1 but not siNEG-treated cultures compared with controls (Figure 6D). These data suggest that TI-VAMP mediates lysosome exocytosis and controls the release of cathepsin B, a soluble luminal material of secretory lysosomes, from glioma cells. Similar inhibition of pro-cathepsin B release was detected in cells treated with h-siRNA 2 (42 $\pm$ 0.8%).

Table 1 | Calcium wave propagation in control and TI-VAMP silenced astrocytes

Distance	Control	r-siRNA	siNEG
Normalised mean peak response (ΔF340/F380)			
At 33 μm	0.91 $\pm$ 0.07	0.86 $\pm$ 0.08	0.89 $\pm$ 0.07
At 66 μm	0.72 $\pm$ 0.053	0.56 $\pm$ 0.08	0.81 $\pm$ 0.08
At 99 μm	0.57 $\pm$ 0.046	0.44 $\pm$ 0.06	0.65 $\pm$ 0.08
At 132 μm	0.51 $\pm$ 0.042	0.33 $\pm$ 0.05	0.51 $\pm$ 0.045
Time to peak (s)			
At 33 μm	0.94 $\pm$ 0.11	1.37 $\pm$ 0.19	0.79 $\pm$ 0.09
At 66 μm	2.05 $\pm$ 0.25	3.04 $\pm$ 0.43	1.44 $\pm$ 0.1
At 99 μm	3.61 $\pm$ 0.29	5.17 $\pm$ 0.46	3.01 $\pm$ 0.25
At 132 μm	6.41 $\pm$ 0.42	8.77 $\pm$ 0.76	5.21 $\pm$ 0.4

Discussion

Astrocytes use secretory lysosomes for ATP release

Secretory lysosomes using TI-VAMP as the SNARE mediating their fusion with the plasma membrane come as the third type of secretory vesicles in astrocytes, besides large dense core vesicles, which store Sg II, ATP and peptides (Calegari et al., 1999; Coco et al., 2003; Pangrsic et al., 2007) and small clear vesicles, which contain and release glutamate and D-serine (Bezzi et al., 2004; Crippa et al., 2006;

Figure 5 | TI-VAMP silencing reduces the amplitude and the speed of calcium wave propagation

(**A** and **B**) Pseudo-colour images of the changes in the calcium concentration (F340/380 signal) in control (**A**) and TI-VAMP silenced (**B**) astrocytes taken 0.5, 2, 4, and 7 s after mechanical stimulation in the presence of 100 μM anandamide. (**C**) Pseudo-colour images of calcium wave propagation at 0.5 and 7 s in astrocytes pre-incubated with the ATP degrading enzyme apyrase (30 μ/mL) and the purinergic receptor antagonist oATP (300 μM). (**D**, **F** and **G**) Temporal analysis of calcium changes of control astrocytes (**F**), astrocytes pretreated with ATP blockers (**D**) and r-siRNA-treated astrocytes (**G**) located 33, 66, 99 and 132 μm far from the stimulated cell shown in A, B and C. (**E** and **F**) Quantitative analysis of the mean calcium responses of astrocytes located at selected distances from the mechanically stimulated cell in control cultures and cultures exposed to ATP blockers (E, $N = 2$ independent experiments, $N = 15$ analysed fields/experiment) or in control cultures and TI-VAMP-silenced cultures (H, $N = 3$ independent experiments, $N = 15$ analysed fields/experiment). Mean peak calcium responses of astrocytes during calcium wave are normalised to calcium response evoked in the mechanically stimulated astrocyte and plotted against distance from the wave centre. Significantly lower calcium responses are detected in r-siRNA-treated astrocytes located 60 and 80 μm far from the wave centre. (**I**) Quantitative analysis of the time to peak of astrocytes at selected distance from the wave center in control and TI-VAMP-silenced cultures. A significant delay in the calcium response was detected in cells located at 99 and 132 μm from stimulated astrocytes. Values are presented as mean $\pm$ SE, obtained from three independent experiments.

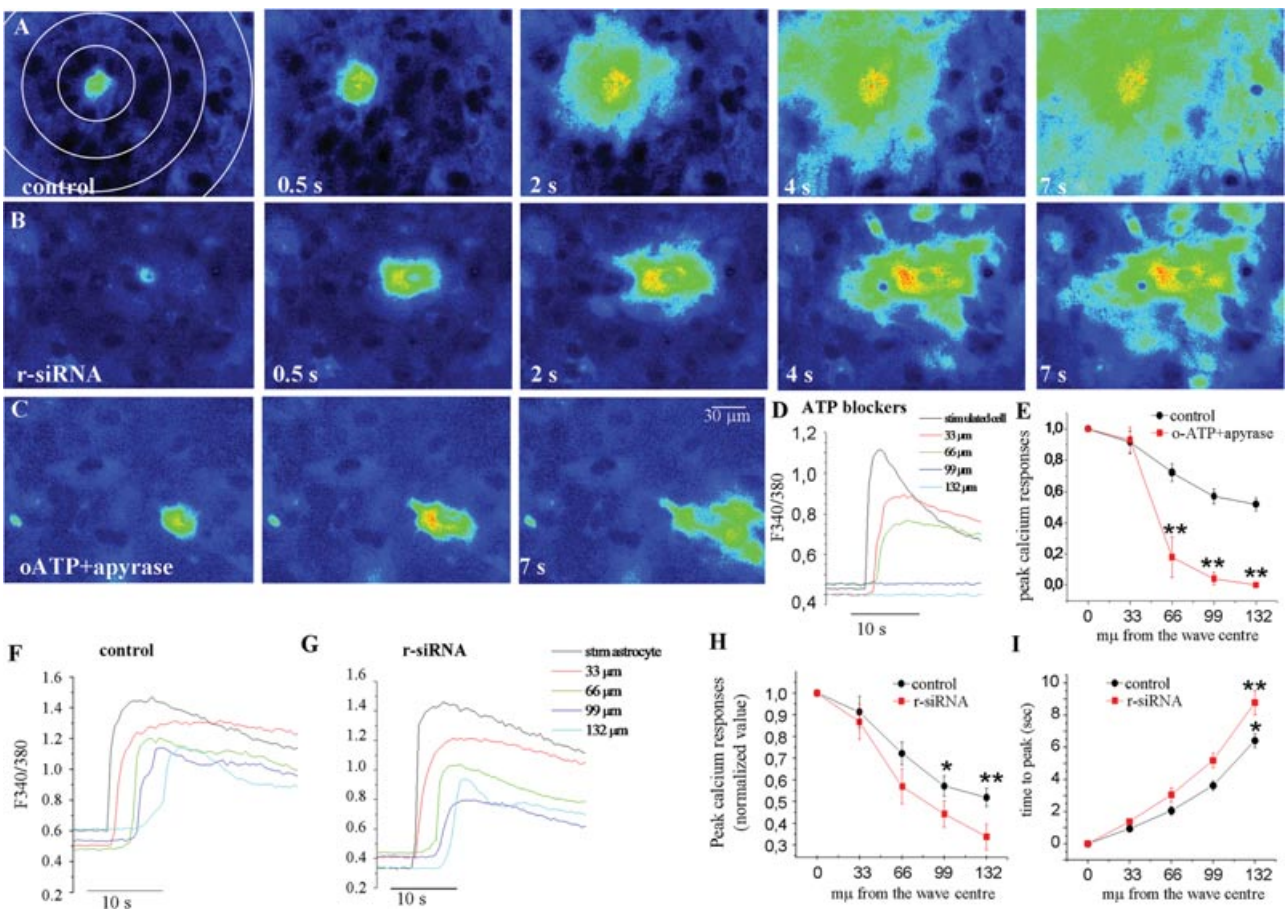

Mothet et al., 2005; Zhang et al., 2004). Electron microscopy analysis of TI-VAMP organelles reveals that these vesicles have a multilamellar appearance, typical of lysosomes, and are characterised by a diameter of 125–175 nm, in the range size of secretory granules (around 115 nm) and larger compared with VAMP2/VAMP3 clear vesicles (30–100 nM).

The molecular analysis of the astrocytic organelles belonging to the different exocytotic routes indicates the involvement of distinct docking and fusion

Figure 6 | Downregulation of TI-VAMP expression reduces pro-cathepsin B secretion from ADF glioma
(**A**) Western blot analysis of TI-VAMP levels in control cultures, and in cultures treated with TI-VAMP h-siRNA1, h-siRNA2 or scrambled oligonucleotides (siNEG) (48 or 96 h, 200 nM). Ribophorin staining guarantees for equal protein loading. (**B** and **C**) Western blot and immunocytochemical staining for TI-VAMP or cathepsin B of ADF cultures treated or not with TI-VAMP h-siRNA1. Scale bar: 25 μm. (**D**) Grey bars, quantitation of pro-cathepsin B detected by ELISA in the supernatant from control or siRNA-treated ADF cells; white bars, TI-VAMP levels measured by western blotting from the same cultures. Note that the heavy reduction of TI-VAMP expression is accompanied by a significant inhibition of pro-cathepsin B secretion. Values are presented as mean $\pm$ SE obtained from five independent experiments in duplicate and are normalised to protein content.

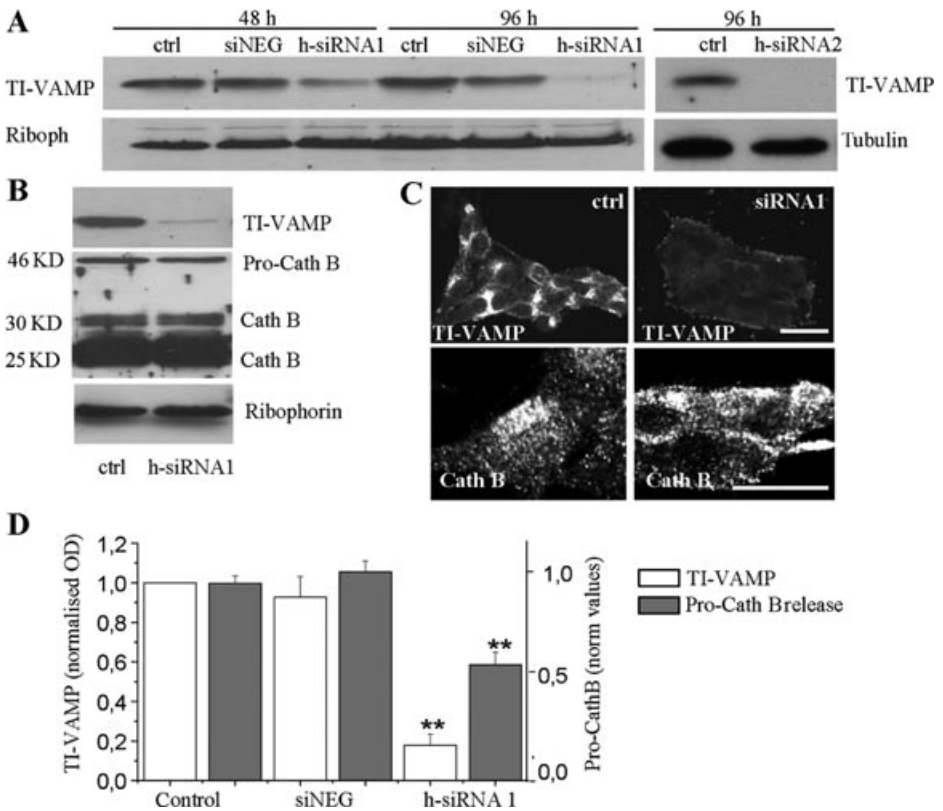

proteins. Indeed, clear glutamatergic vesicles contain VAMP2, VAMP3 and are devoid of TI-VAMP and rab7 (Crippa et al., 2006). Conversely, although subcellular fractions enriched in TI-VAMP organelles largely overlap with fractions positive for secretory granules, immunoisolation of TI-VAMP organelles reveals their lysosomal nature; indeed, TI-VAMP multilamellar organelles are positive for the late endosomes/lysosomes marker rab7 and are devoid of the early endosomal markers rab5 and TrfR (this study), suggesting that they likely correspond to secretory lysosomes. Secretory lysosomes, first identified in cells of haematopoietic origin, are multilamellar/dense core structures, which share many traits with conventional lysosomes and secretory granules, as they are acidic and contain degradative proteins but also can undergo regulated secretion (Luzio et al., 2007). Recently, lysosomes, labelled by prolonged incubation with FM dyes, able to undergo both partial and full calcium-dependent exocytosis, have been identified in astrocytes (Jaiswal et al., 2007; Li et al., 2008; Zhang et al., 2007). In glial cells, secretory lysosomes can be loaded with the fluorescent ATP analogue Mant-ATP and release it upon stimulation. In addition, lysosome-enriched subcellular fractions contain ATP, indicating that lysosomes could be a source of vesicular ATP release from astrocytes (Zhang et al., 2007), besides secretory granules (Coco et al., 2003; Pangrsic et al., 2007). Exocytotic release of ATP from secretory granules was indicated by the presence of

ATP in Sg II-enriched subcellular fractions and inhibition of ATP release by tetanus toxin (Coco et al., 2003) or by a dominant negative of VAMP2 (Pangrsic et al., 2007; Pascual et al., 2005). The finding that inhibition of ATP release occurs upon VAMP2 inactivation represents an indisputable proof that a fraction of ATP is localised in a vesicular compartment, distinct from TI-VAMP vesicles, which fuse with the plasma membrane using the tetanus toxin-sensitive SNARE VAMP2. However, consistent with the presence of ATP also in secretory lysosomes (Jaiswal et al., 2007; Li et al., 2008; Zhang et al., 2007) and in line with TI-VAMP representing the SNARE of secretory lysosomes in astrocytes (this study), we describe a high degree of co-localisation between TI-VAMP and either the ATP analogue Mant-ATP or quinacrine, which labels ATP-containing organelles. More importantly, we show that exocytosis of quinacrine-positive vesicles as well as calcium wave propagation, the latter reflecting ATP release, are significantly inhibited in TI-VAMP-silenced cultures. A direct demonstration of TI-VAMP involvement in ATP release is provided by luciferin–luciferase experiments. These results represent the first evidence that functional impairment of the TI-VAMP secretory pathway results in decreased ATP exocytosis from astrocytes, providing the final demonstration that ATP is stored in two distinct vesicular organelles, Sg II and VAMP2-positive secretory granules and TI-VAMP-positive secretory lysosomes, from which it is released by regulated calcium-dependent exocytosis (Halassa and Haydon, 2010; Hamilton and Attwell, 2010; Parpura and Zorec, 2010).

TI-VAMP mediates cathepsin release from glioma

In line with their identity as secretory lysosomes, TI-VAMP organelles highly co-localise with the late endosome/lysosomes marker CD63 and contain in their lumen the lysosomal cysteine protease cathepsin B in ADF glioma. Cathepsin B is highly upregulated in malignant tumours and its release into the extracellular medium as inactive precursor of 42 kDa, as well as in its active mature forms of 31–33 kDa and 26–24 kDa, is critical for glioma dissemination in the brain (Rao, 2003). Indeed, cathepsin B directly participates to tissue destruction and indirectly contributes to extracellular matrix degradation by enhancing the activity of metalloproteinases. The present study, by identifying TI-VAMP as the v-SNARE which mediates cathepsin B release by secretory lysosomes, opens a new strategy for limiting tumour invasiveness, based on the silencing of the v-SNARE. Reducing cathepsin B release, but leaving invariate its expression within tumour cells, may have significant advantages relative to cathepsin B silencing, as cathepsin B activates cell death, when released from lysosomes into the cytosol (Foghsgaard et al., 2001; Werneburg et al., 2002, 2004). Therefore, downregulation of TI-VAMP expression might allow to limit the invasive potential of glioma, while maintaining the potential of the enzyme to induce apoptosis in tumour cells.

Materials and methods

Cell cultures

All experimental procedures were in strict accordance with the Italian and European Union regulation on animal welfare and were authorised by the Italian Ministry of Health. Hippocampal or cortical glia cultures were obtained from embryonic rat Sprague–Dawley pups (E18) using previously described methods (Calegari et al., 1999). Briefly, after dissection, the hippocampi/cortices were dissociated by treatment with trypsin (0.25% for 15 min at 37°C), followed by fragmentation with a fire-polished Pasteur pipette. Dissociated cells were plated on either glass coverslips or tissue culture dishes at a density of 0.5×10^6 cells/mL of glial medium: minimal essential medium (Invitrogen) supplemented with 20% fetal calf serum (Euroclone) and glucose at a final concentration of 5.5 g/L. To obtain a pure astrocyte monolayer, any microglial cells were harvested by shaking 3-wk-old cultures.

Immunohistochemistry on brain slices

Double immunofluorescent labelling on brain slices were performed on vibratome sections obtained from two rat foetuses at embryonic day E16 (Sprague–Dawley; Charles River). All the experiments were undertaken in accordance with the guidelines established in the Principles of Laboratory Animal Care (directive 86/609/EEC). The embryos obtained from anaesthetised pregnant rat (4%; 1 mL/100 g body weight, intraperitoneal; post-natal rats) were anaesthetised with ether and perfused with mixed aldehydes (Ortino et al., 2003). Free-floating sections were first incubated in 10% albumin from bovine serum albumin (BSA) and 0.2% Triton-X100 in phosphate-buffered saline (PBS), pH 7.4 for 1 h and then incubated overnight at 4°C in a mixture of polyclonal TI-VAMP (1:100) and monoclonal anti-Vimentin antibodies (1:200), in 1% BSA in PBS. After several rinse in PBS, sections were incubated in a mixture of the corresponding secondary antibodies: biotinylated goat anti-rabbit antibody (1:200, Vector Laboratories) and fluorescein isothiocyanate (FITC)-conjugated horse anti-mouse antibody (1:100, Jackson Immunoresearch Laboratories) followed by an incubation in rhodamine red-conjugated streptavidin (1:200, Jackson Immunoresearch Laboratories). Sections were mounted in Fluor-Save (Calbiochem) and examined with a confocal laser scanning microscope (Bio-Rad) equipped with argon/krypton mixed gas

laser and mounted on a light microscope (Eclipse E600; Nikon). Confocal images were recorded through separate channels at the excitation peaks 510 nm (for FITC) and 550 nm (for rhodamine red-conjugated streptavidin) to avoid cross-talk and were merged with Bio-Rad Lasersharp 2000 software.

siRNA treatment and transfection

ADF glioma cells were trypsinised 6 h before transfection and transfected using lipofectamine reagent (Invitrogen) according to the manufacturer's instructions. After 48 h, a further siRNA transfection was performed and cell were monitored after 2 days.

Small interfering RNA experiments were carried out using siRNA duplex oligoribonucleotides designed to be selective for human TI-VAMP. Stealth oligo sequences (Invitrogen) h-siRNA 1 were as follows:

(sense) UGA AGA ACC UCA AGC UCA CUA UUA U;
(antisense) AUA AUA GUG AGC UUG AGG UUC UUC A.

Stealth oligo sequences (Invitrogen) h-siRNA 2 were as follows:

(sense) GAU UCU GGC UAA GAU ACC UUC UGA A
(antisense) UUC AGA AGG UAU CUU AGC CAG AAU C.

A similar protocol was used to transfect hippocampal astrocytes with oligo sequences (HP GenomeWide siRNA Quiagen Rn_RGD:621558_1) selective for rat TI-VAMP, r-siRNA:

(sense) GCA AUU AUU UGU UUC ACU ATT
(antisense) UAG UGA AAC AAA UAA UUG CCA.

Negative control stealth oligo sequences, siNEG, (Invitrogen) were as follows:

(sense) UGA AAC CCU AAC GCU CAA UUG AUA U
(antisense) AUA UCA AUU GAG CGU UAG GGU UUC A.

In rescue experiments, astrocytes were transfected by Amaxa, according to the manufacturer's instructions, with r-siRNA alone or with r-siRNA in combination with cDNA encoding for human TI-VAMP-EGFP (Martinez-Arca et al., 2000) (accession number of the human TI-VAMP sequence: http://www.ncbi.nlm.nih.gov/nuccore/NM_005638.5).

After 48 h, a further siRNA transfection using lipofectamine reagent was performed and ATP release from control astrocytes, r-siRNA silenced cells transfected or not with human TI-VAMP-GFP was carried out 2–3 days later.

The sequences were designed to minimise homology to any known vertebrate transcript and did not induce the interferon-mediated stress response pathways, according to the manufacturer's specifications. Optimisation of siRNA design was carried out with BLAST analysis (National Centre for Biotechnology Information; http://www.ncbi.nlm.nih.gov/BLAST).

For immunocytochemistry, astrocytes were trypsinised 1 day before transfection. Cells were transfected using Fugene reagent (Roche) according to the manufacturer's instructions and monitored after 2–3 days. cDNA encoding Cellubrevin–GFP was described by Martinez-Arca et al., 2003.

Immunofluorescence and electron microscopy

For double immunofluorescence, cells were incubated in 120 mM phosphate buffer, pH 7.2, containing 4% formaldehyde and 4% sucrose. After fixation, cells were immunostained using primary antibodies followed by the appropriate secondary antibodies, as described previously (Calegari et al., 1999). Secondary antibodies were from Jackson Immunoresearch Laboratories. Coverslips were mounted in the mounting medium for fluorescence Vectashield (Vector Laboratories). Images were acquired using a Bio-Rad MRC-1024 confocal microscope equipped with LASERSHARP 3.2 software. To quantify the co-localisation of TI-VAMP with various cellular markers, optical sections were analysed using the co-localisation plug in of ImageJ software (http://rsb.info.nih.gov/ij).

Lysotracker live staining was performed by incubating ADF glioma cells for 60 min at 37°C with medium containing 60 nM Lysotracker-RED DND-99. Cells were washed three times with KRH and fluorescence acquired with a Leica SP5 confocal microscope. Quinacrine staining was performed by incubating living hippocampal astrocytes for 30 min at 37°C with KRH containing 0.5 μM quinacrine dihydrochloride (Sigma). After washing, cells were incubated with 10 μM FM 4-64 and immediately acquired with a Leica SP5 confocal microscope. Electron microscopy of entire cells was performed as described previously (Calegari et al., 1999). Briefly, after fixation, astrocytes were scraped from the dishes and pelleted in an Eppendorf centrifuge. The pellets were dehydrated and infiltrated in Epon 812 for preparation of plastic sections. Sections were cut on a Reichert Ultracut E microtome, counterstained and examined with a Philips CM10 electron microscope.

Subcellular fractionation and TI-VAMP-positive vesicle isolation

Astrocytes or ADF were grown on Petri dishes until near confluence, harvested by scraping, washed and resuspended in homogenisation buffer [10 mM HEPES–KOH, pH 7.4, 250 mM sucrose, 1 mM magnesium acetate, protease inhibitor cocktail (1:1000 P8340 Sigma)]. The cells were homogenised using a cell cracker (European Molecular Biology Laboratory) and centrifuged at 1000*g* for 10 min to prepare the post-nuclear supernatant. This supernatant was loaded on a 0.4–1.8 M continuous sucrose gradient and spun in a SW41 rotor (Beckman Instruments) at 80,000*g* for 18 h. Fractions of 1 mL were collected and analysed by SDS-PAGE followed by western blotting as previously described (Calegari et al., 1999; Coco et al., 2003). TI-VAMP-positive vesicles were immunoisolated from a post-nuclear supernatant of cultured hippocampal astrocytes with Dynabeads M-280 (Invitrogen) sheep anti-rabbit IgG1 coupled to polyclonal antibody anti-TI-VAMP, according to the manufacturer's instructions. Bound vesicles were either further analysed by SDS-PAGE and western blotting or processed for electron microscopy. For the latter, the beads were fixed with 2.5% glutaraldehyde in 0.1 M cacodylate buffer, pH 7.4, overnight at 4°C and after several washes in cacodylate buffer were post-fixed with 2% OsO_4 for 2 h. Samples were dehydrated in a graded ethanol series and embedded in EPON (Fluka) epoxy resin. Sections were cut on a Reichert Ultracut E microtome, counterstained and examined with a Philips CM10 electron microscope. Vesicle diameters were evaluated on images at 52,500× final magnification.

Isolation of magnetic early and late endocytic compartments

Nanoparticles (synthesized at PECSA, University Pierre et Marie Curie–CNRS UMR 7195 Paris, France) are made of a metallic core of maghemite (γ-Fe_2O_3), with diameter 8 nm, and bear negative surface charges because of carboxylate groups complexed on their surface, ensuring their stability in aqueous solution. Magnetic labelling of the ADF cells was performed by adding to the cell medium (supplemented with 5 mM citrate) a filter-sterilised suspension of magnetic nanoparticles at an extracellular iron concentration of 5 mM, for 30 min. The cells were then washed and incubated for 30 min or 6 h to permit nanoparticle internalisation and confinement within early or late endosomes/lysosomes, respectively. After washing in HB buffer (250 mM sucrose, 5 mM imidazole, pH 7.4, 5 mM MgSO4, 1 mM ethylenediaminetetraacetic acid, 0.5 mM ethylene glycol-bis(beta-aminoethyl ether)-N,N,N′,N′-tetra acetic acid (EGTA), 0.15 mg/mL casein), cells were scraped from the plastic support, centrifuged and resuspended in HB buffer supplemented with 1-mM DTT and protease inhibitor cocktail. They were then homogenised by passing them several times through a 23-G needle. Unbroken cells and nuclei were removed from the cell homogenate by centrifugation at 1300*g* for 7 min, and the post-nuclear supernatant was loaded onto a syringe fixed to a magnet. After overnight incubation at 4°C, the subcellular compartments containing magnetic nanoparticles accumulated on the side of the syringe fixed to the magnet and were collected and analysed by SDS-PAGE and western blotting.

Time-lapse TIRF imaging

In TIRF imaging experiments, at which we monitored secretory events, quinacrine fluorescence signal was measured in individual cells, in basal conditions and upon stimulation with t-ACPD. t-ACPD stimulation was also carried out in astrocytes previously treated with r-siRNA for TI-VAMP. To prevent photobleaching of the sample, TIRF imaging was used in real time and images were acquired for only 40 ms in 250 ms intervals. The analysis was restricted to few ROIs per cell located in different areas of the cells. Only when quinacrine fluorescence increased, spread and then declined below the basal level, the event counted as a secretory event. In dual-wavelengths recording, we imaged quinacrine/TI-VAMP co-localisation signals in sequential mode under evanescent fields' illumination. In TIRF imaging experiments, at which we monitored $[Ca^{2+}]_i$ surrounding the fusing vesicles, spread intensity of X-rod fluorescence was analysed to regions (8 μm^2) surrounding quinacrine-labelled vesicles. Light was filtered with dual-band filter sets and fluorescence images were visualised using a CCD camera Hamamatsu 9100-02 EM-CCD. In all TIRF imaging experiments, the laser beam was tilted at a specific critical angle to obtain total internal reflection at the glass–cell interface according to Snell's law. The refractive indices for glass ($n = 1.52$ at 488 nm) and cells ($n = 1.38$) predict an evanescent field in which excitation of the fluorophores is varied from 70 to 110 nm in thickness (Leica AM TIRF MC). Video images were analysed with Leica AF7000 software.

Analysis of calcium wave propagation

Cultured hippocampal astrocytes were loaded with 2 μM Fura-2 pentacetoxy methylester for 45 min at 37°C in Krebs–Ringer solution buffered with HEPES (KRH; 125 mM NaCl, 5 mM KCl, 1.2 mM $MgSO_4$, 2 mM $CaC1_2$, 10 mM glucose and 25 mM HEPES/NaOH, pH 7.4) and transferred to the recording chamber of an inverted microscope (Axiovert 100TV; Zeiss) equipped with a calcium imaging unit. Polychrome IV (TILL Photonics, Germany) was used as light source. Fura-2 fluorescence images were collected with a CCD camera Imago-QE (Till Photonics), and analyzsd with the Tillvision 4.0.1 software. Images were acquired at 2–4 ratio/s. To evoke calcium wave propagation, astrocytes were mechanically stimulated with a glass pipette mounted on a micromanipulator. The pipette tip was placed directly above one cell and the microelectrode was advanced and retracted rapidly to mechanically stimulate the astrocyte. The average intensity of the propagated calcium wave was calculated by plotting the peak calcium response of a given astrocyte against its distance from the centre of the wave. Calcium transients of the most responsive cells in the field at selected distance from the centre of the wave (33, 66, 99, 132 μm) were normalised to the response of the stimulated astrocyte. The average speed of calcium wave propagation was calculated by plotting the time to peak of astrocytes involved in the wave against the distance from the centre of the wave (33, 66, 99, 132 μm from the stimulated astrocyte). All calculations and graphs were done using Origin 6.0 Software and the results were expressed as means $\pm$ SE. Consistent imaging settings were used across experimental conditions and individual experiments (e.g. frame rates, exposure times, etc.).

ATP bioluminescence assay

ATP levels in the extracellular saline (KRH) of astrocyte monolayers, stimulated for 5 min with 1 μM bradikinin in the presence of the ecto-ATPase inhibitor ARL (10 μM), were measured using a luciferi–/luciferase-based ATP determination kit (Molecular Probes, Leiden, NL) and a luminometer (Lumat, Berthold, LB9501) according to the manufacturer's instructions. Each sample was run in triplicate. Samples were assayed within 5 min of collection.

Chemicals

Antibodies against VAMP7/TI-VAMP, SNAP-23, cellubrevin/VAMP3 and CD63 were produced by T. Galli (INSERM, Paris). Antibodies against Tom20 were purchased by Santa Cruz Biotech. Anti-vimentin antibodies were from Dako. Antibodies against syntaxin 1-3, α-tubulin, Rab7, catalase and calnexin were from Sigma. Antibodies against VAMP2 were from Synaptic System. Antibodies against human cathepsin B were from Calbiochem and Chemicon. Antibody against EAA1 was from BD. Antibody anti-Sg II was a kind gift of P. Rosa (CNR Institute of Neuroscience, Milan, Italy). Antibodies against ribophorin were kindly provided by G. Kreibich (New York University). Antibody directed against the human TfR was a kind gift from I. Trowbridge (Salk Institute). Anti-Rab5 antibodies were kindly provided by R. Jahn (Max-Planck-Institute for Biophysical Chemistry). ATP, ionomycin, anandamide, apyrase, oATP, quinacrine dihydrochloride and ARL were from Sigma. Mant-ATP Lysotracker-RED DND-99 and FM 4-64 were from Molecular Probes.

Data analysis

The data are presented as means $\pm$ SE. Statistical significance was evaluated by the Student's test or one-way analysis of

variance. Differences were considered significant if $p<0.05$ and are indicated by an asterisk in all figures, whereas those at $p<0.01$ are indicated by double asterisks.

Author contribution

C.V. carried out experimental work, contributed to design research and wrote the article; M.B., C.C., L.R., U.S., C.F., E.Z., L.D., M.F. and A.C. carried out experimental work and analysed data; C.W. provided reagents; T.G. and M.C. contributed to design research and data interpretation; M.M. devised the concept, contributed to design research and wrote the article.

Funding

This work was supported by Cariplo 2008-3104 (to M.M.), FISM 2010/R/39 (to C.V.), Progetto CIPE/Limonte (to M.C.) and in part by grants from INSERM (Avenir Program), the European Commission 'Signalling and Traffic' [STREP 503229], the Association pour la Recherche sur le Cancer, the Agence Nationale pour la Recherche 'Astrex', the Mairie de Paris Medical Research and Health Program, the Fondation pour la Recherche Médicale (to T.G.). L.D. was supported by Association pour la Recherche sur le Cancer and by the Agence Nationale pour la Recherche.

Acknowledgements

We thank Dr Flavia Antonucci (University of Milan), Dr Raffaella Morini (University of Milan), Valentina Cappello (University of Milan) and Giuliana Fossati for help in some experiments and Dr Elisabetta Menna and Dr Romana Tomasoni (DIBIT HSR) for discussion. We also thank Dr Francesca Aloisi (Istituto Superiore di Sanità, Rome) for providing primary human astrocytes.

Conflict of interest statement

The authors have declared no conflict of interest.

References

Advani, R.J., Yang, B., Prekeris, R., Lee, K.C., Klumperman, J. and Scheller, R.H. (1999) VAMP-7 mediates vesicular transport from endosomes to lysosomes. J. Cell Biol. **146**, 765–776

Bezzi, P., Gundersen, V., Galbete, J.L., Seifert, G., Steinhauser, C., Pilati, E. and Volterra, A. (2004) Astrocytes contain a vesicular compartment that is competent for regulated exocytosis of glutamate. Nat. Neurosci. **7**, 613–620

Bianco, F., Perrotta, C., Novellino, L., Francolini, M., Riganti, L., Menna, E., Saglietti, L., Schuchman, E.H., Furlan, R., Clementi, E., Matteoli, M. and Verderio, C. (2009) Acid sphingomyelinase activity triggers microparticle release from glial cells. EMBO J. **28**, 1043–1054

Bucci, C., Thomsen, P., Nicoziani, P., McCarthy, J. and van Deurs B. (2000) Rab7: A key to lysosome biogenesis. Mol. Biol. Cell **11**, 467–480

Calegari, F., Coco, S., Taverna, E., Bassetti, M., Verderio, C., Corradi, N., Matteoli, M. and Rosa, P. (1999) A regulated secretory pathway in cultured hippocampal astrocytes. J. Biol. Chem. **274**, 22539–22547

Caplan, S., Hartnell, L.M., Aguilar, R.C., Naslavsky, N. and Bonifacino, J.S. (2001) Human Vam6p promotes lysosome clustering and fusion *in vivo*. J. Cell Biol. **154**, 109–122

Casey, T.M., Meade, J.L. and Hewitt, E.W. (2007) Organelle proteomics: Identification of the exocytic machinery associated with the natural killer cell secretory lysosome. Mol. Cell Proteomics **6**, 767–780

Coco, S., Calegari, F., Pravettoni, E., Pozzi, D., Taverna, E., Rosa, P., Matteoli, M. and Verderio, C. (2003) Storage and release of ATP from astrocytes in culture. J. Biol. Chem. **278**, 1354–1362

Crippa, D., Schenk, U., Francolini, M., Rosa, P., Verderio, C., Zonta, M., Pozzan, T., Matteoli, M. and Carmignoto, G. (2006) Synaptobrevin2-expressing vesicles in rat astrocytes: Insights into molecular characterization, dynamics and exocytosis. J. Physiol. **570**, 567–582

Evanko, D.S., Zhang, Q., Zorec, R. and Haydon, P.G. (2004) Defining pathways of loss and secretion of chemical messengers from astrocytes. Glia **47**, 233–240

Fellin, T. (2009) Communication between neurons and astrocytes: Relevance to the modulation of synaptic and network activity. J. Neurochem. **108**, 533–544

Foghsgaard, L., Wissing, D., Mauch, D., Lademann, U., Bastholm, L., Boes, M., Elling, F., Leist, M. and Jäättelä, M. (2001) Cathepsin B acts as a dominant execution protease in tumor cell apoptosis induced by tumor necrosis factor. J. Cell Biol. **153**, 999–1010

Halassa, M.M. and Haydon, P.G. (2010) Integrated brain circuits: Astrocytic networks modulate neuronal activity and behavior. Annu. Rev. Physiol. **72**, 335–355

Hamilton, N.B. and Attwell, D. (2010) Do astrocytes really exocytose neurotransmitters? Nat. Rev. Neurosci. **11**, 227–238

Hepp, R., Perraut, M., Chasserot-Golaz, S., Galli, T., Aunis, D., Langley, K. and Grant, N.J. (1999) Cultured glial cells express the SNAP-25 analogue SNAP-23. Glia **27**, 181–187

Hur, Y.S., Kim, K.D., Paek, S.H. and Yoo, S.H. (2010) Evidence for the existence of secretory granule (dense-core vesicle)-based inositol 1,4,5-trisphosphate-dependent Ca^{2+} signaling system in astrocytes. PLoS One **5**, e11973

Jaiswal, J.K., Fix, M., Takano, T., Nedergaard, M. and Simon, S.M. (2007) Resolving vesicle fusion from lysis to monitor calcium-triggered lysosomal exocytosis in astrocytes. Proc. Natl. Acad. Sci. U. S. A. **104**, 14151–14156

Li, D., Ropert, N., Koulakoff, A., Giaume, C. and Oheim, M. (2008) Lysosomes are the major vesicular compartment undergoing Ca2+-regulated exocytosis from cortical astrocytes. J. Neurosci. **28**, 7648–7658

Logan, M.R., Lacy, P., Odemuyiwa, S.O., Steward, M., Davoine, F., Kita, H. and Moqbel, R. (2006) A critical role for vesicle-associated membrane protein-7 in exocytosis from human eosinophils and neutrophils. Allergy **61**, 777–784

Loubery, S., Wilhelm, C., Hurbain, I., Neveu, S., Louvard, D. and Coudrier, E. (2008) Different microtubule motors move early and late endocytic compartments. Traffic **9**, 492–509

Luzio, J.P., Pryor, P.R. and Bright, N.A. (2007) Lysosomes: Fusion and function. Nat. Rev. Mol. Cell Biol. **8**, 622–632

Martineau, M., Galli, T., Baux, G. and Mothet, J.P. (2008) Confocal imaging and tracking of the exocytotic routes for D-serine-mediated gliotransmission. Glia **56**, 1271–1284

Martinez-Arca, S., Alberts, P., Zahraoui, A., Louvard, D. and Galli, T. (2000) Role of tetanus neurotoxin insensitive vesicle-associated membrane protein (TI-VAMP) in vesicular transport mediating neurite outgrowth. J. Cell Biol. **149**, 889–900

Martinez-Arca, S., Proux-Gillardeaux, V., Alberts, P., Louvard, D. and Galli, T. (2003) Ectopic expression of syntaxin 1 in the ER redirects TI-VAMP- and cellubrevin-containing vesicles. J. Cell Sci. **116**, 2805–2816

Montana, V., Malarkey, E.B., Verderio, C., Matteoli, M. and Parpura, V. (2006) Vesicular transmitter release from astrocytes. Glia **54**, 700–715

Mothet, J.P., Pollegioni, L., Ouanounou, G., Martineau, M., Fossier, P. and Baux, G. (2005) Glutamate receptor activation triggers a calcium-dependent and SNARE protein-dependent release of the gliotransmitter D-serine. Proc. Natl. Acad. Sci. U. S. A. **102**, 5606–5611

Oishi, Y., Arakawa, T., Tanimura, A., Itakura, M., Takahashi, M., Tajima, Y., Mizoguchi, I. and Takuma, T. (2006) Role of VAMP-2, VAMP-7, and VAMP-8 in constitutive exocytosis from HSY cells. Histochem. Cell Biol. **125**, 273–281

Ortino, B., Inverardi, F., Morante-Oria, J., Fairen, A. and Frassoni, C. (2003) Substrates and routes of migration of early generated neurons in the developing rat thalamus. Eur. J. Neurosci. **18**, 323–332

Paco, S., Margeli, M.A., Olkkonen, V.M., Imai, A., Blasi, J., Fischer-Colbrie, R. and Aguado, F. (2009) Regulation of exocytotic protein expression and Ca2+-dependent peptide secretion in astrocytes. J. Neurochem. **110**, 143–156

Pangrsic, T., Potokar, M., Stenovec, M., Kreft, M., Fabbretti, E., Nistri, A., Pryazhnikov, E., Khiroug, L., Giniatullin, R. and Zorec, R. (2007) Exocytotic release of ATP from cultured astrocytes. J. Biol. Chem. **282**, 28749–28758

Parpura, V. and Zorec, R. (2010) Gliotransmission: Exocytotic release from astrocytes. Brain Res. Rev. **63**, 83–92

Pascual, O., Casper, K.B., Kubera, C., Zhang, J., Revilla-Sanchez, R., Sul, J.Y., Takano, H., Moss, S.J., McCarthy, K. and Haydon, P.G. (2005) Astrocytic purinergic signaling coordinates synaptic networks. Science **310**, 113–116

Proux-Gillardeaux, V., Raposo, G., Irinopoulou, T. and Galli, T. (2007) Expression of the Longin domain of TI-VAMP impairs lysosomal secretion and epithelial cell migration. Biol. Cell **99**, 261–271

Pryazhnikov, E. and Khiroug, L. (2008) Sub-micromolar increase in [Ca(2+)](i) triggers delayed exocytosis of ATP in cultured astrocytes. Glia **56**, 38–49

Pryor, P.R., Mullock, B.M., Bright, N.A., Lindsay, M.R., Gray, S.R., Richardson, S.C., Stewart, A., James, D.E., Piper, R.C. and Luzio, J.P. (2004) Combinatorial SNARE complexes with VAMP7 or VAMP8 define different late endocytic fusion events. EMBO Rep. **5**, 590–595

Ramamoorthy, P. and Whim, M.D. (2008) Trafficking and fusion of neuropeptide Y-containing dense-core granules in astrocytes. J. Neurosci. **28**, 13815–13827

Rao, J.S. (2003) Molecular mechanisms of glioma invasiveness: the role of proteases. Nat. Rev. Cancer **3**, 489–501

Rao, S.K., Huynh, C., Proux-Gillardeaux, V., Galli, T. and Andrews, N.W. (2004) Identification of SNAREs involved in synaptotagmin VII-regulated lysosomal exocytosis. J. Biol. Chem. **279**, 20471–20479

Sander, L.E., Frank, S.P., Bolat, S., Blank, U., Galli, T., Bigalke, H., Bischoff, S.C. and Lorentz, A. (2008) Vesicle associated membrane protein (VAMP)-7 and VAMP-8, but not VAMP-2 or VAMP-3, are required for activation-induced degranulation of mature human mast cells. Eur. J. Immunol. **38**, 855–863

Schubert, V., Bouvier, D. and Volterra, A. (2011) SNARE protein expression in synaptic terminals and astrocytes in the adult hippocampus: A comparative analysis. Glia **59**, 1472–1488

Striedinger, K., Meda, P. and Scemes, E. (2007) Exocytosis of ATP from astrocyte progenitors modulates spontaneous $Ca2^{+}$ oscillations and cell migration. Glia **55**, 652–662

Werneburg, N.W., Guicciardi, M.E., Bronk, S.F. and Gores, G.J. (2002) Tumor necrosis factor-α-associated lysosomal permeabilization is cathepsin B dependent. Am. J. Physiol. Gastrointest. Liver Physiol. **283**, G947–G956

Werneburg, N.W., Guicciardi, M.E., Yin, X.M. and Gores, G.J. (2004) TNF-alpha-mediated lysosomal permeabilization is FAN and caspase 8/Bid dependent. Am. J. Physiol. Gastrointest. Liver Physiol. **287**, G436–G443

Zhang, Q., Fukuda, M., Van Bockstaele, E., Pascual, O. and Haydon, P.G. (2004) Synaptotagmin IV regulates glial glutamate release. Proc. Natl. Acad. Sci. U. S. A. **101**, 9441–9446

Zhang, Z., Chen, G., Zhou, W., Song, A., Xu, T., Luo, Q., Wang, W., Gu, X.S. and Duan, S. (2007) Regulated ATP release from astrocytes through lysosome exocytosis. Nat. Cell Biol. **9**, 945–953

Received: 5 July 2011; Accepted: 5 December 2011; Accepted article online: 7 December 2011